First International Conference on
Microchannels and Minichannels
April 24-25, 2003, Rochester, New York, USA
1ICMM2003-1110

DISPENSING PICOLITER DROPLETS USING DIELECTROPHORETIC (DEP) MICRO-ACTUATION

R. Ahmed, D. Hsu, C. Bailey, and T.B. Jones
Department of Electrical and Computer Engineering
University of Rochester
Email: r*ajib@ece.rochester.edu*

Nomenclature

A_x = cross-sectional area of moving finger
C_d = dielectric capacitance (F)
C_w = water capacitance (F)
d = dielectric coating thickness
D = spacing between two electrodes (m)
D_d = diameter of sessile droplets (μm)
E = electric field (V/m)
f^e = electrical force
f_d = drag force
f_γ = surface tension force
g = terrestrial acceleration (m/s^2)
g = gap between parallel electrode strips
G = geometric parameter (D/R)
G_w = conductance of water (S)
h_{DEP} = dielectric height of rise
K = voltage coefficient
K = complete elliptical integral
k^2 = $[g/(g + 2\delta w)]^2$
P_f = oil/water perimeter
R_{calc} = calculated radius
s = spacing between droplets
t = time (seconds)
V = applied voltage (V-rms)
V^* = threshold voltage (V-rms)
w = electrode width (μm)
$Z(t)$ = length of finger (mm)
δw = overlap of water droplet (μm)
ε_0 = permittivity of free space (F/m)
ε_w = dielectric permittivity of water
κ_1 = dielectric constant of Pellat's liquid
λ_c = critical wavelength (μm)
λ^* = most unstable wavelength (μm)
μ = dynamic viscosity of water
ρ = density of Pellat's dielectric liquid
ρ_w = density of water
σ_W = conductivity of water (S/m)
τ_d = viscous shear stress

Abstract

Non-uniform, AC electric fields created by co-planar electrode strips patterned on an insulating substrate are used to move and manipulate aqueous liquid masses, and to dispense very small droplets. This liquid dielectrophoretic microactuation scheme has potential applications for microfluidic systems in the laboratory on a chip. This dispensing system uses the electrodes to draw a long finger or rivulet of liquid from the parent microliter droplet. We propose and provide data that supports a very simple power law dependence of the finger length upon time: $Z(t) \propto \sqrt{t}$, which governs the time required to fill a structure. Microliter-sized, sessile water droplets are divided into large numbers of droplets down to ~40 picoliters when the voltage is removed. The breaks up of the rivulet into droplets is a result of the familiar capillary instability. The hydrodynamic instability features a critical wavelength, below which instability is not possible, and a most unstable wavelength, which controls the volume and spacing of the droplets formed.

Introduction

Liquid dielectrics, including water, respond to a non-uniform, AC electric field by collecting preferentially in regions of strong field intensity. We exploit this phenomenon, liquid dielectrophoresis (DEP), using simple, co-planar electrodes patterned on insulating substrates in a microfluidic scheme to transport and manipulate small deionized water inventories very rapidly. These electrode structures can be used to form arrays of droplets averaging less than ~40 picoliters

starting from a single microliter droplet dispensed from a micropipette. Application of the voltage distributes the liquid rapidly in a rivulet or finger atop the electrode structures in <0.1 sec. The finger breaks up into the droplets by action of capillary instability, which proceeds, also rapidly, once the voltage is turned off. Refer to Fig. 1. The droplet spacings are controlled by the fastest growing unstable wavelength, whereas the volumes are determined by the width of the structures and to some extent, the filling time.

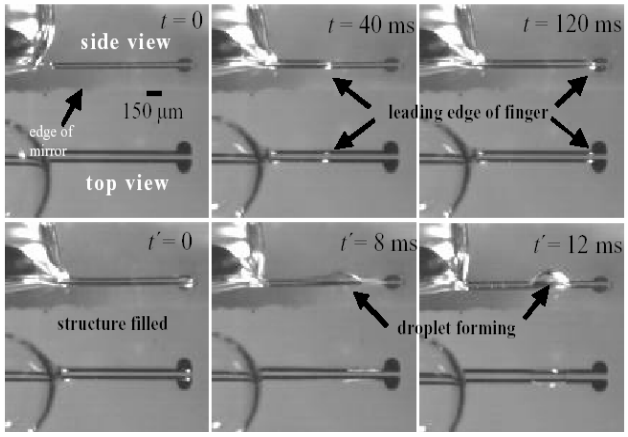

Fig 1. Frames from a video sequence taken at 250 fps showing side (using a 55º mirror) and top views of finger motion from left to right, when the voltage is turned on, and then droplet formation due to the capillary instability, when the voltage is turned off. Note the droplet shape. Droplet formation takes ~1/10 the time required for the finger to reach the end of the 3 mm long structure.

Dielectrophoresis (DEP) is an example of the ponderomotive effect, the basis of which is the force exerted on dipoles by a non-uniform electric field [1].

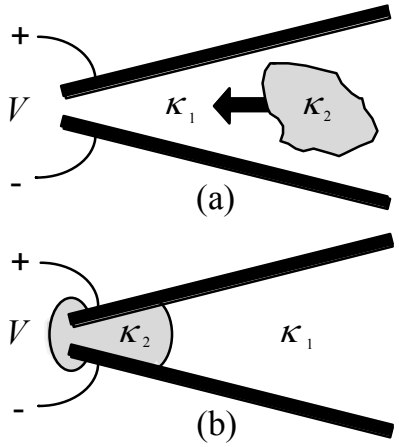

Fig 2. Critical phenomenology of liquid dielectrophoresis (DEP). (a) A liquid of dielectric constant $\kappa_2 > \kappa_1$ is drawn into region of strong electric field. (b) In the preferred hydrostatic equilibrium, the dielectric liquid surface conforms to the electric field lines.

The dipoles -- individual molecules in the case of a liquid -- tend to collect in regions of high electric field intensity as shown in Fig. 2a. This same force repels gas or vapor bubbles within this liquid from strong fields. Ordinarily, the preferred equilibrium of the collected liquid fixes the liquid surface to be parallel with the electric field lines, as depicted in Fig. 2b.

Liquid DEP differs from other electrohydrodynamic (EHD) phenomena used in microfluidic systems (such as the ion-drag effect, electroconvection, and electro-osmosis) in that it is not a true pumping mechanism. Instead, the non-uniform electric field, created by the electrodes, establishes a hydrodynamic equilibrium that the liquid rushes to fill when voltage is applied. Once the equilibrium is reached, flow stops. Pellat's classic demonstration of liquid DEP, shown in Fig. 3, consists of two plane, parallel electrodes at spacing D, oriented vertically and partially immersed in a pool of dielectric liquid of mass density ρ, and dielectric constant κ_1 [3]. Gas of negligible density and polarizability approximately equal to free space, $\varepsilon_o = 8.854\times10^{-12}$ F/m, covers the liquid. For an applied voltage, the static dielectric height of rise is

$$h_{\mathrm{DEP}} = \frac{\varepsilon_o(\kappa-1)E^2}{2\rho g} \qquad (1)$$

where $E \approx V/D$ is the uniform electric field between the plates, V is the applied voltage, and g = 9.81 m/s^2 is the terrestrial acceleration due to gravity.

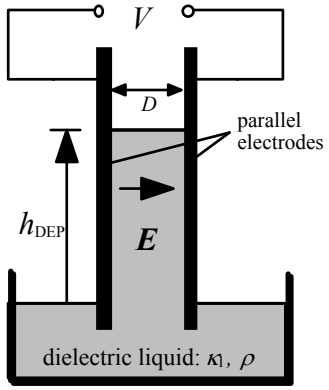

Fig 3. Original experiment of Pellat with two parallel, vertically oriented uncoated electrodes partially immersed into a pool of dielectric liquid.

Though liquid DEP and electrowetting are closely related electromechanical effects [4], there are important distinctions. Electrowetting manifests itself as a change in the contact angle of a sessile droplet of conductive

liquid placed on top of a metallic electrode covered with a thin dielectric layer. The contact angle decreases as voltage is increased, resulting in a decrease of the interfacial force between the droplet and the solid substrate. As a consequence, the conductive droplet will spread over the surface appearing to be more hydrophilic in nature. In electrowetting, DC or low frequency AC (typically ≤1 kHz) is used and the electric field does not penetrate the liquid. To exploit the electrowetting effect in microfluidic applications, aqueous liquid is introduced between dielectric-coated, parallel electrodes spaced ~100 μm to 1000 μm apart. One of the electrodes is usually made of glass coated with a conductive layer, such as indium/tin oxide [5, 6].

Experimental

The electrodes used for DEP microactuation are usually co-planar strips made of vapor-deposited aluminum with an approximate thickness of ~2kÅ patterned on a glass substrate [7]. These electrodes are spin-coated uniformly with a dielectric material such as Teflon AF™ or SU-8™ to avoid boiling and electrolysis. We apply a very thin layer of photoresist, Shipley 1805™ (average thickness ≤1 μm), on top of the dielectric coatings to make the surface of the substrate somewhat hydrophobic. Joule heating can be a major drawback when we apply high voltage but immersing the substrates

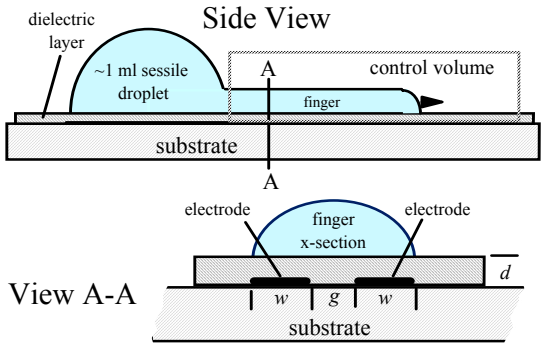

Fig. 4 Side view and cross-section (View A-A) of transient DEP actuation using parallel, co-planar electrodes. The motion is transient and ceases when the liquid reaches the end of the electrodes opposite the sessile droplet. The non-uniform electric field confines the footprint of the finger to a width of approximately $2w + g$.

in oil alleviates this problem. The oil helps dissipate heat by thermal conduction across the liquid/liquid interface. In preparation for individual experiments, a ~1 microliter droplet of deionized water ($\sigma_w \sim 10^{-6}$ S/cm) is deposited at one end of the electrodes. When sufficient voltage is applied, a finger of liquid emerges from the sessile droplet and rushes toward the other end. Refer to Fig. 4. After the finger reaches the other end of the electrodes, the transient flow ceases and a hydrostatic equilibrium in the shape of a long rivulet held in place by the non-uniform electric field is established. View A-A of the figure shows a schematic representation of the cross section of the finger and the co-planar electrode strips of width w, spacing g, and negligible thickness. Our observation is that the cross-section of the advancing finger is flatter and thinner toward its leading edge, but fills in and quickly assumes a nearly semi-circular profile.

Dynamics of finger motion

Two principal mechanisms control the DEP droplet dispenser: (i) the initial transient motion of the finger in response to application of the voltage and (ii) formation of the droplets by action of the capillary instability. In both regimes, fairly simple predictive models seem to describe the observed behavior.

Model for finger dynamics

Consider a liquid finger of length $Z(t)$ emerging from a sessile droplet and moving along the electrodes as shown in Fig. 4. Writing the momentum conservation expression for a control volume containing the entire finger yields:

$$\frac{d}{dt}\left[(\rho A_x) Z \frac{dZ}{dt}\right] = f^{\mathrm{e}} + f_\gamma + f_{\mathrm{d}} \qquad (2)$$

In Eq. (2), $f^{\mathrm{e}} = KV^2$ is the DEP force. If we assume that the liquid profile is constant along the length of the finger except at its leading edge, then a simple electromechanical model may be used to determine that $K \propto dC/dZ$, where $C(Z)$ is the system capacitance, a function of the finger length. Because C is a linear function of finger length Z, dC/dZ = constant, so f^{e} is also constant. Note that this result would also be obtained by using the Maxwell Stress Tensor on the appropriate control volume [13]. Derivation of the electrical force f^{e} using this method shows that the origin of this force does not depend on the details of the field at the leading edge of the finger. The surface tension term $f_\gamma \approx -\gamma P_f$, where γ is the sum of oil-water interfacial tension and solid-liquid surface tension, and P_f is fluid/fluid (oil/water) perimeter, is roughly constant and retards the motion. Finally, there is the fluid drag force $f_{\mathrm{d}} \approx -(P_f + 2w + g) Z(t) \tau_{\mathrm{d}}$, where τ_{d} is the viscous

shear stress which depends on the finger velocity, dZ/dt .

Eq. (2) can be simplified by recognizing that, even for the rapid transient flows we observe, the momentum term is insignificant on all important time scales and may be ignored. Both the electrical and surface tension forces are constant; only the drag depends on time. If we further assume $\tau_d = \mu G dZ/dt$, the equation of motion reduces to

$$\frac{dZ^2}{dt} = \frac{2(KV^2 - \gamma P_f)}{\mu G(P_f + 2w + g)} \tag{3}$$

Applying the initial condition $Z(t = 0) = 0$, the solution is

$$Z(t) = A\sqrt{t} \tag{4}$$

where the coefficient A is:

$$A = \sqrt{\frac{2(KV^2 - \gamma P_f)}{\mu G(P_f + 2w + g)}} \tag{5}$$

Even without detailed knowledge of some of the parameters in Eq. (5), such as K, G, and P_f, most of the important parametric dependencies of A are still evident.

The simple analysis leading to Eq. (4) is open to criticism on several counts. For example, the coefficients K and G, and the perimeter P_f, used to define f^e, f_d, and f_γ, are taken to be constant in time. Furthermore, the formulation for the drag force may be criticized as too simplistic. Other loss mechanisms that we have ignored, principally related to wetting, may contribute to impeding the motion of the finger. With our present experimental apparatus, however, it is not possible to investigate and determine such wetting effects. Nevertheless, the model does take into account the most important features of the transient flow, in particular, the dependence of the viscous drag upon the length of the finger. Examining the expression for A, one notes that the model accounts for the competition between the electrical and surface tension forces, predicting a voltage threshold for actuation that is consistent with experimental observation. It should be noted that the same, simple "square root" law, $Z(t) \propto \sqrt{t}$ has been invoked successfully elsewhere, namely, in the description of certain thermocapillary flows that have compelling similarities to DEP microactuation [7].

Finger dynamics data

We have studied the transient dynamics of water fingers using a high-speed video camera to capture the motion as a function of time. To investigate the motion, finger length data were extracted from every 5th frame from videos all recorded at 500 fps. Fig. 5 shows typical kinetic data. These and other data sets from similar experiments have been analyzed using regression analyses based on the square root law to yield a value for A, and associated confidence limits based on Student's t-distribution statistics [9]. The curve plotted in Fig. 5 is the best-fit square root law for the data.

Values for A and associated 99% confidence intervals are tabulated in Table I. For the wider electrode structures tested (w = g = 20 μm), A exhibits strong dependence on the voltage. Increasing the voltage from 200 to 325 V-rms increases the mean values of A by a factor of more than three. This behavior is at least consistent with the voltage dependence evident in Eq. (5) if one assumes that the voltage threshold for motion in not too much below the value of 200 V. Because of the high interfacial tension as well as solid-liquid surface tension that the water droplet has to overcome prior to actuation, a simple linear relationship is not evident between A and V when the applied voltage is just above the threshold, $\left(V^* = \sqrt{\frac{\gamma P_f}{K}}\right)$ value. A linear relationship between A and V should only emerge when V is much higher than V^*. Probably due to variability in wetting conditions on our dielectric coatings, we have not yet been able to measure voltage thresholds reliably, but we are convinced that the values for the 20 μm structures tested are somewhere between 100 and 200 V-rms. Limited data obtained with smaller electrode structures (w = 10 μm, g = 20 μm) is also presented. Comparable values of A with these smaller structures demonstrate that the coefficient is not

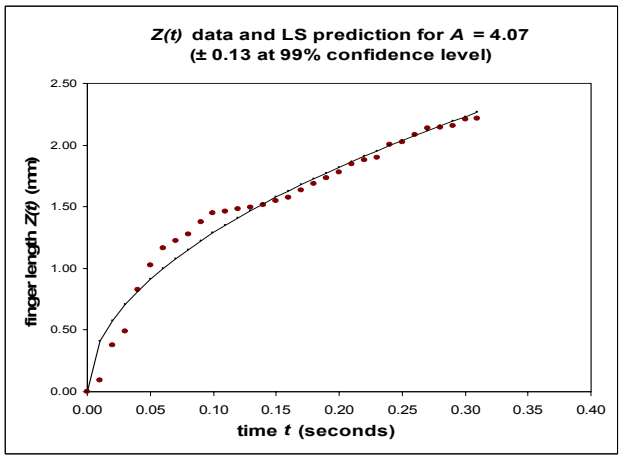

Fig.5. Finger length $Z(t)$ versus time t for a 3 mm long structure with w = g = 20 μm. Applied voltage was 200 V-rms at 50 kHz. Experiment was performed in oil bath.

as strongly dependent on the width of the structures as it is on the applied voltage although for a smaller structure, the mean values of A should be higher, as reflected in the table.

Frequency effects

As mentioned earlier, liquid DEP is a strong function of the electric field frequency. There is a critical frequency threshold above which the electric field penetrates the liquid and influences the finger's cross-sectional profile. *Jones et al.* presented a simple RC circuit model to estimate the minimum frequency required for a semi-circular profile [7]:

Table I. Values of the coefficient A defined in Eq. (5) and computed from least-squares analysis of finger length $Z(t)$ versus time t data for co-planar electrode structures. The ± limits for A are obtained using Student's t-distribution statistics at the 99% confidence level.

Electrode dimensions (in μm)	Voltage V (Volts-rms)	Frequency f (in kHz)	mean A (with 99% confidence limits)
w = 20 g =20	200	50	4.07 ± 0.13
same	200	50	4.72 ± 0.24
same	225	100	4.6 ± 0.41
same	325	100	19.67 ± 1.47
same	325	100	17.3 ± 1.71
same	375	200	17.13 ± 2.91
same*	300	100	4.83 ± 0.18
same *	400	200	4.56 ± 0.21
w = 10 g =20	275	100	16.73 ± 0.5
same	275	100	16.81 ± 0.56
same	275	100	17.06 ± 0.52

*.. Different dielectric coating material was used to extract data with these electrodes. We believe surface wetting conditions are responsible for this anomaly in A values as different dielectric coating materials have different threshold voltage requirement.

$$f_c = \frac{G_w}{2\pi(\frac{C_d}{2} + C_w)} \qquad (6)$$

where $$G_w = \frac{\sigma_w \mathrm{K}(1-k^2)}{2\mathrm{K}(k^2)}$$

and $$C_d = \frac{\varepsilon_0 \delta w}{t},\ C_w = \frac{\varepsilon_w}{\sigma_w} G_w$$

C_d is the capacitance of the dielectric layer, ε is the dielectric permittivity, and $\delta w = (w+g/2)$ is the overlap of the water droplet. K is the complete elliptical integral of the first kind with argument $k^2 = [g/(g + 2\delta w)]^2$, while σ_w and ε_w are the conductivity and dielectric permittivity of the water, respectively. For the three sizes of structures tested, from the largest to the smallest, respectively, the critical frequency values are calculated to be 20, 21 and 22 kHz. The critical frequency is much more strongly dependent on the thickness of the dielectric coating t, than on width w.

The A values depend on frequency as well as the voltage as long as the voltage is well above the threshold value but this dependence is negligible. Comparing two data points at (200 V, 50 kHz) and (225 V, 100 kHz) one notes virtually no change in A. This result indicates that A is not strongly dependent on frequency at least in the range of frequencies tested. We can also observe that

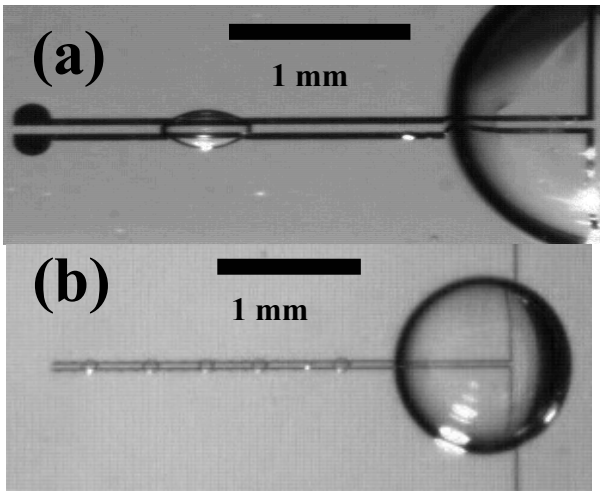

Fig 6. Droplet formation in co-planar DEP structures. (a) Larger structure: w = 50 μm, g = 50 μm, length = 3 mm). (b) Smaller structure: w = 20 μm, g = 20 μm, length = 3 mm, with 6 droplets with average volume ~200 (S.D.=± 48) picoliters.

beyond 100 kHz, there is no further increase in A values, even if the voltage is increased. It is interesting to note that the mean value of A does not depend strongly on structure width, as both 20 and 10 μm structures give comparable values at 100 and 200 kHz.

Despite deficiencies in the assumptions and approximations used to obtain the $Z(t) \propto \sqrt{t}$ law for water finger dynamics, the model provides a useful predictive relationship for length versus time when voltage is applied. Simple scaling considerations may be based on this model. For example, doubling the length will increase the filling time by a factor of four. Values for the coefficient A derived from the data generally reflect the expected voltage and cross-sectional scale dependences as well as surface wetting conditions. More

data and better control of wetting are needed to perform a fuller evaluation of the model.

Droplet formation dynamics

Until the voltage is removed, the finger -- either moving or stationary -- is maintained in stable hydrodynamic or hydrostatic equilibrium by the non-uniform electric field of the co-planar electrodes. The rivulet configuration becomes unstable immediately when voltage is removed. This instability is very much like the capillary jet instability familiar from ink-jet printers, flow cytometers, and liquid spraying. The difference is that, in our systems, the liquid is in contact with the substrate and it forms a regular array of sessile droplets distributed along the electrode structure. No electrical force is present during droplet formation; however, surface wetting conditions are very influential. We have also found that the overall width, ($2w$+g), and also the shape of the electrode strips influence droplet volume and the locations where they form. For example, for our wider structures (w, $g \geq 50$ μm), few droplets tend to form, apparently because much of the liquid inventory of the finger is drawn rapidly back into the parent droplet when voltage is removed. In Fig. 6a, a single droplet, representing only ~27% of the original finger volume, is formed. On the other hand, in the narrower structure shown in Fig 6b, six droplets of average volume ~200 picoliters, totaling to ~33% of the original finger volume, have formed.

Regularly spaced, semi-circular bumps, as shown in Fig. 7, have been used successfully to form uniformly spaced droplets with ±20% volume uniformity [7]. If the spacing between any two subsequent bumps is too large, satellite droplets form between them. Bumps have little influence on the wavelength of the capillary instability, but they help to initiate formation if the spacing is correctly chosen. To gain a better understanding of the factors influencing droplet formation in DEP structures, we carried out basic studies of the phenomenon in narrow structures without bumps.

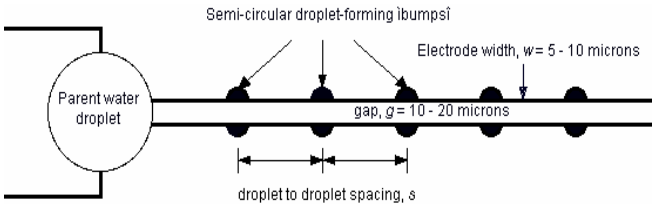

Fig. 7. Electrode strips with periodic semicircular bumps intended to fix the location of the droplets that form when the voltage is removed.

Capillary instability of a rivulet

Rayleigh's classical theory for the hydrodynamic instability of a free circular jet of radius R predicts that disturbances at all wavelengths greater than $\lambda_c = 2\pi R$ are unstable, and that those at wavelength $\lambda^* = 9.016R$ will grow fastest [10]. Davis developed a linearized model for the capillary instability of a uniform rivulet, accounting for wetting along the contact line of the liquid by hypothesizing and testing various wetting and/or pinning constraints imposed as boundary conditions [11]. For all cases considered, instability was predicted above some wavelength, except for the case of fixed contact angle and then only when the contact angle is less than 90°. Schiaffino and Sonin [12] extended this linearized model to predict the most unstable wavelengths for each of the contact line constraints investigated by Davis.

The difficulty in using the rivulet models of either Davis or Schiaffino and Sonin in our experiments is that the contact line constraint is unknown. While the electric field is on, the contact line of the finger seems to be pinned almost directly above the edges of the electrodes by local field intensification. Also, we observe the contact angle of the liquid to be close to 90° above the critical electric field frequency f_c. This is probably because the electric field lines, *which penetrate the liquid in DEP actuation*, are constrained to be perpendicular at the surface of the electrodes. But the governing condition at the contact line when the electric field is removed is not known. The instability evolves far too rapidly for our present video recording capability. Furthermore, the contact line is quite difficult to see anyway, so we have not yet made any definitive observations.

Droplet spacing and size data

To study the capillary instability of these artificial rivulets, we have recorded the spacings and radii of the sessile droplets formed after DEP actuation. Data have been obtained from electrode structures with the same cross-sectional dimensions used in the finger dynamics studies, viz., w = 20 μm, g = 20 μm and w = 10 μm, g = 15 μm. Fig. 8 shows an experiment conducted with one of the narrower structures, 6 mm long, which produced ~30 droplets of average volume of ~40 (S.D.=±10) picoliters at an average spacing of 160 (S.D.=±54) μm. According to Rayleigh's theory, using $R = w + g/2$, the most unstable wavelength for a cylindrical jet is 158 μm.

This correspondence encouraged more detailed analysis of the data.

Each droplet in images like Fig. 8 can be treated as an opportunity to test whether or not the finger cross-section is uniform. We first assume that the finger profile is semicircular with some radius R_{calc} and that the droplets are hemispherical with diameter D_d. Equating the volume of each droplet to the presumed volume of liquid in the finger that was used to form it, we get:

$$\pi/2\, R_{calc}^2\, s = \pi/12\, D_d^3 \qquad (7)$$

which one may re-arrange to obtain an expression for the apparent finger radius that depends only on the measurable quantities and D_d:

$$R_{calc} = \sqrt{D_d^3/6\, s} \qquad (8)$$

Fig. 9 plots calculated values of the apparent finger radius R_{calc} using data from Fig. 8. There is considerable scatter in these data, but a typical average value is 11 (±4) μm, which is in reasonable agreement with $R = w + g/2$ = 17.5 μm. The fact that R_{calc} is smaller than R suggests that the profile is flattened, instead of semicircular. Video images indicate that the *moving* finger is tapered and thinner at its leading edge. We did linear regression analyses on several data sets to determine if the R_{calc} values reflect this taper by decreasing with distance from the parent droplet, but found none. Such a result may mean only that the flow had stopped by the time the voltage was turned off.

Conclusion

DEP microactuation uses simple co-planar electrodes patterned on an insulating substrate to manipulate small volumes of liquid, including aqueous solutions. Applications in microfluidic systems intended for the laboratory on a chip are envisioned. One important capability of DEP microfluidics is the dispensing of multiple droplets down to 40 picoliters starting directly from microliter-sized, sessile parent drops deposited manually on the substrate with a micropipette. The dispensing process occurs in two stages. First, the electrodes are energized with AC voltage (200 to 400 V-rms), causing a narrow finger of liquid to flow from the parent droplet. The motion of the leading edge of this finger seems to obey a square root law, that is, $Z(t) \propto \sqrt{t}$. The finger (or rivulet) remains a hydrodynamically stable configuration as long as the non-uniform field is present; but when the field is removed, capillary instability immediately breaks the rivulet into droplets. Raleigh's hydrodynamic model for predicting the most unstable wavelength was successfully implemented to determine the spacing between any two subsequent droplets. A reasonable correspondence

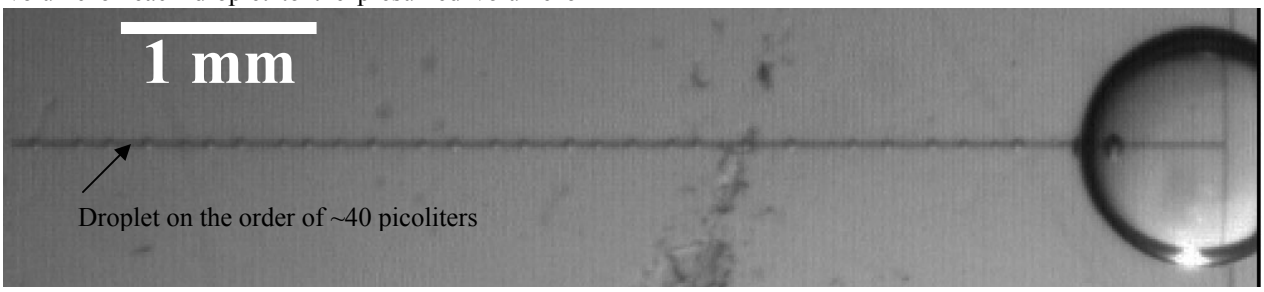

Fig 8. Simultaneous formation of multiple droplets using an electrode structure with w = 10 μm, g = 15 μm, and length = 6 mm. Upon application of 400 V-rms @ 100 kHz, the finger filled in <0.1 seconds. Approximately 30 droplets, of average volume of 40 (S.D.=±10) picoliters and average spacing of 160 (S.D.=±54) μm, were produced.

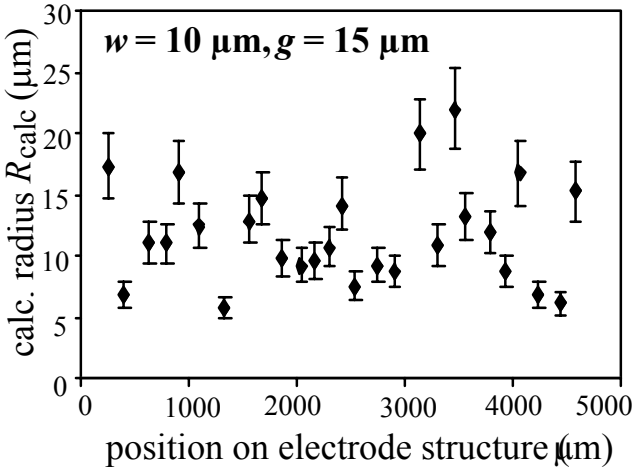

Fig. 9. Calculated values of apparent finger radius R_{calc}, obtained from measured diameters D_d and spacings s of individual droplets along electrode structures. The error bars indicate estimated measurement uncertainties for the droplet diameters (±15%) and their spacings (±15%).

between the theoretical value and the experimental data was observed.

References

[1] R. Becker, Electromagnetic Fields and Interactions (Dover: New York) 1964, §37.

[2] T.B. Jones and J.R. Melcher, 1973 *Phys. Fluids* 16, 393-400.

[3] H. Pellat, 1894 *C.R. Seances Acad. Sci.* (Paris) **119** 675.

[4] T.B. Jones, 2000 *Langmuir* **18** 4437-4443.

[5] M.G. Pollack, R.B. Fair, A.D. Shenderov, 2000 *Applied Physics Lett*. **77**, 1725-1726.

[6] J. Lee, H. Moon, J. Fowler, T. Schoellhammer, and C-J. Kim, 2002 *Sensors Actuators A* **95**, 259-268.

[7] T.B. Jones, M. Gunji, M. Washizu, M.J. Feldman, 2001 *J. Appl. Phys*. **89** 1441.

[8] A.A. Darhuber, S.M. Troian, W.W. Reisner, 2001 *Phys. Rev. E* **64**, .

[9] A.D. Rickmers, H.N. Todd, Statistics: an Introduction, (McGraw-Hill: New York) 1967, chapter. 12.

[10] J.W.S. Rayleigh, The Theory of Sound vol. 2 (Dover Pub.: New York) 1945, §359.

[11] S.H. Davis, 1980 *J. Fluid Mech.* 98 225-242.

[12] S. Schiaffino and A.A. Sonin, *J. Fluid Mech.* 343 95-110 (1997).

[13] H. H. Woodson and J. R. Melcher, Electromechanical Dynamics (pt. 2), (Wiley: New York) 1968, Chapter 8.